Clinical and Experimental Gastroenterology

Dovepress
Taylor & Francis Group

Open Access Full Text Article

ORIGINAL RESEARCH

Therapeutic Effects and Mechanisms of Faecalibacterium Prausnitzii in a Rat Model of Liver Cirrhosis

Xinjun Hu[1,2,*], Chengyu Ma[1,*], Bingyou Yin[1], Yafeng Liu[1], Bingyang Shang[1], Yibing Shang[1], Fenzhi Ji[1], Yingjian Zhang[2,3]

[1]Department of Infectious Diseases, The First Affiliated Hospital, College of Clinical Medicine, Henan University of Science and Technology, Luoyang, People's Republic of China; [2]Department of Gastroenterology, The First Affiliated Hospital, College of Clinical Medicine, Henan University of Science and Technology, Luoyang, People's Republic of China; [3]Henan Medical Key Laboratory of Gastrointestinal Microecology and Hepatology, Luoyang, People's Republic of China

*These authors contributed equally to this work

Correspondence: Xinjun Hu; Yingjian Zhang, Email hxj5129@163.com; zhangyingjian@haust.edu.cn

Background and Aims: Liver cirrhosis development is often accompanied by dysbiosis of the intestinal flora. As an important component of the human intestinal microflora, *Faecalibacterium prausnitzii* plays an important role in maintaining the intestinal ecological balance. This study aimed to investigate the protective effect of *F. prausnitzii* on carbon tetrachloride-induced cirrhosis in rats and its effect on intestinal homeostasis.

Methods: A rat model of liver cirrhosis was generated via treatment with CCL4 and gavage with *F. prausnitzii* live bacterial solution. Samples of blood, liver, colon and feces were collected from the rats. Liver function, serum cytokine levels, liver and intestinal pathology, the fecal flora structure and liver transcriptomics were assessed in the rats.

Results: *F. prausnitzii* administration attenuates pathological damage to the liver in cirrhotic rats; reduces the serum levels of alanine aminotransferase (ALT), aspartate aminotransferase (AST), total bilirubin (TB), alkaline phosphatase (ALP) and direct bilirubin (DB) ($p < 0.05$, $p < 0.01$); increases the albumin (ALB) level ($p < 0.05$); downregulates the expression of tumor necrosis factor-alpha (TNF-α), interleukin-6 (IL-6), IL-10, IL-1β ($p < 0.05$, $p < 0.01$) and interferon-gamma (IFN-γ) ($p < 0.05$); reduces damage to the intestinal mucosal structure in cirrhotic rats; and maintains the barrier function of the intestine. In cirrhotic rats, certain organisms exhibited a decrease in abundance, while others showed an increase.

Conclusion: *F. prausnitzii* administration had a protective effect on cirrhotic rats by effectively regulating the intestinal flora, enhancing the barrier function of the intestinal tract, inhibiting the inflammatory response of the liver, and delaying liver fibrosis. This study provides a theoretical basis for the clinical application of *F. prausnitzii*.

Keywords: liver cirrhosis, Faecalibacterium prausnitzii, intestinal homeostasis, liver function

Introduction

Cirrhosis, the end stage of chronic liver disease, is a progressive disease caused by a variety of factors, including chronic hepatitis B and C viral infections, nonalcoholic fatty liver disease (NAFLD), alcohol-related liver disease, and autoimmune diseases.[1] Globally, it has a high mortality rate, seriously endangering human life and health and representing an enormous health burden on society.[2]

The pathogenesis of cirrhosis is deeply intertwined with the dysfunction of the gut-liver axis, a critical bidirectional communication network between the hepatic and intestinal systems. Within this framework, a clearly defined vicious cycle—"cirrhosis-intestinal flora imbalance-inflammation"—perpetuates disease progression.[3] This cycle initiates as liver impairment disrupts bile acid metabolism and systemic circulation, compromising intestinal barrier integrity and fostering a state of dysbiosis. Characteristic alterations include a decrease in beneficial genera such as Anaplasma and

Received: 3 July 2025
Accepted: 11 December 2025
Published: 19 December 2025

Bifidobacterium, alongside an increase in potentially pathogenic taxa like Streptococcus and Enterobacteriaceae.[3–5] A compromised intestinal barrier facilitates the translocation of bacterial products, particularly pathogen-associated molecular patterns (PAMPs) such as lipopolysaccharides, into the portal circulation.[6] Upon reaching the liver, these PAMPs activate Kupffer cells and hepatic stellate cells primarily via Toll-like receptors (TLRs), triggering a robust pro-inflammatory response through NF-κB signaling and leading to the sustained production of cytokines, including tumor necrosis factor (TNF-α), interleukin-6 (IL-6), and transforming growth factor-β1 (TGF-β1).[6,7] This persistent inflammation not only directly exacerbates hepatocyte apoptosis and fibrosis but also further disrupts host metabolism, thereby reinforcing the initial dysbiosis and closing the self-amplifying loop.[8]

A key microbial player implicated in the stability of the gut-liver axis is *Faecalibacterium prausnitzii*, one of the most abundant commensal bacteria in the healthy human gut and a prominent member of the Firmicutes phylum.[9] Current research firmly establishes *F. prausnitzii* as a pivotal anti-inflammatory bacterium. Its depletion is a common feature in various chronic inflammatory conditions, including inflammatory bowel disease (IBD) and, notably, cirrhosis, suggesting its potential role as a guardian against gut-liver axis disruption.[4,10] The mechanisms underlying its beneficial effects are twofold. First, it is a major producer of butyrate, a short-chain fatty acid that serves as the primary energy source for colonocytes, crucially strengthens the intestinal epithelial barrier, and possesses direct anti-inflammatory properties.[10] Second, it exerts immunomodulatory effects, such as promoting the regulatory T cell (Treg)/T helper 17 (Th17) balance towards an anti-inflammatory state, thereby helping to control both intestinal and systemic inflammation.[11,12] Given these attributes, *F. prausnitzii* has emerged as a leading next-generation probiotic candidate.

However, direct evidence demonstrating that supplementing with *F. prausnitzii* can specifically break the "cirrhosis-dysbiosis-inflammation" cycle remains limited. Therefore, this study was designed to explore the protective effects of *F. prausnitzii* administration in a rat model of carbon tetrachloride-induced cirrhosis, with a specific focus on its impact on intestinal homeostasis and the underlying mechanisms, as investigated through 16S rRNA gene sequencing and hepatic transcriptomics.

Materials and Methods

Strains and Culture Conditions

F. prausnitzii (DSM107838) was obtained from the German Collection of Microorganisms and Cell Cultures GmbH (DSMZ). The purchased strain was anaerobically incubated with the prepared modified *Clostridium fortuitum* liquid medium in an anaerobic incubator at 37 °C for 24 h. The liquid medium was centrifuged at 4000 rpm for 10 min, and bacteria were obtained by discarding some of the supernatant. The bacteria were washed twice with saline and resuspended to a concentration of 1×10^9 colony-forming units (CFUs)/mL in physiological medium. All methods were carried out in accordance with relevant guidelines and regulations. The study was approved by the Ethics Committee of the First Affiliated Hospital, College of Clinical Medicine, Henan University of Science and Technology (2019G-015).

Experimental Design and Model of Cirrhosis

Eighteen male Sprague–Dawley rats (6–8 weeks of age, 200–250 g) were randomly divided into three groups: a negative control group treated with saline (NC group), a CCL4-induced cirrhosis model group treated with saline (CCL4 group) and a CCL4-induced cirrhosis model group treated with *F. prausnitzii* (*F. prausnitzii* group). Treatment and modeling schedule: the experimental timeline is summarized in Figure 1. All gavage treatments were administered once daily during the pre-modeling phase (week 0–1) and twice weekly thereafter (week 1–14). Cirrhosis was induced in the Model and treatment groups by intraperitoneal (i.p). injection of 50% CCl_4 (in olive oil) at a dose of 0.5 mL/kg twice per week starting from day 8. The NC group received i.p. injections of an equivalent volume of olive oil at the same frequency. After 14 weeks of modeling, all treatments were stopped for one week before the rats were euthanized for analysis. All experimental procedures complied with the requirements of the Guidelines for the Care and Use of Laboratory Animals of the National Institutes of Health of China in 2012 and were approved by the Ethics Committee of the First Affiliated Hospital of Henan University of Science and Technology.

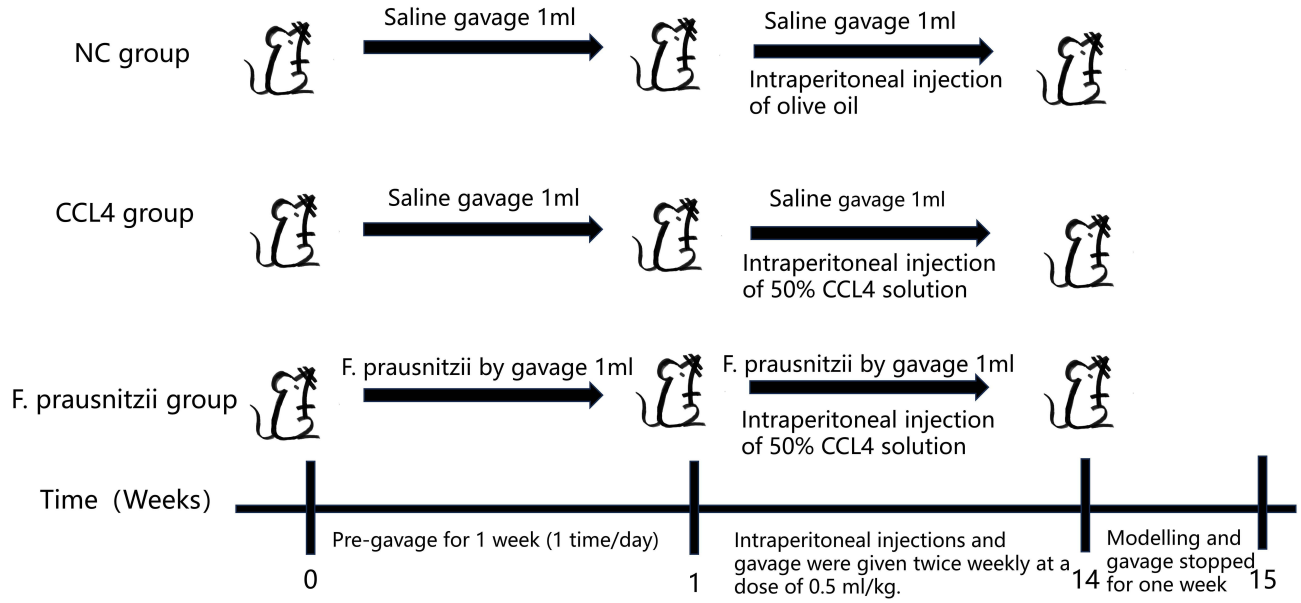

Figure 1 The construction process of mouse model: The process of constructing the normal control group, the CCL4 treatment group and *F. prausnitzii* group. All groups were subjected to the following procedures: From week 0 to week 1 (pre - gavage period), intragastric administration was performed once a day for 1 week. From week 1 to week 14, intraperitoneal injection and intragastric administration were given twice a week at a dose of 0.5 mL/kg. From week 14 to week 15, modeling and gavage were stopped for 1 week. It is dealt with as follows: NC group: Intragastric administration of 1 mL saline (twice) and intraperitoneal injection of olive oil; CCl4 group: Intragastric administration of 1 mL saline (twice) and intraperitoneal injection of 50% CCl4 solution; *F. prausnitzii* group: Intragastric administration of 1 mL *F. prausnitzii* bacterial solution (twice) and intraperitoneal injection of 50% CCl4 solution.

Abbreviations: NC group, Normal control group; CCl4 group, Carbon tetrachloride-induced liver injury model group; *F. prausnitzii* group, *Faecalibacterium prausnitzii* intervention group.

Biochemical Indicators of Liver Function

The serum levels of alanine aminotransferase (ALT), aspartate aminotransferase (AST), alkaline phosphatase (ALP), total bilirubin (TB), direct bilirubin (DB), albumin (ALB), alkaline phosphatase (ALP) and γ-glutamyltransferase (GGT) were assessed via standard methods via a 7600–210 automatic analyzer (Hitachi 7600–210; Hitachi, Tokyo, Japan).

Liver and Spleen Index Assessment

At the end of the experiment, the rats were euthanized, and their livers/spleens were immediately excised and weighed. The liver/spleens index was calculated as follows: Liver/spleen index (%) = (Liver/spleen weight / Final body weight) × 100%.

Cytokine Analysis

Serum was obtained from abdominal aortic blood samples collected under anesthesia. Following coagulation, samples were centrifuged at 3000 rpm (approximately × g) for 15 minutes at 4°C to isolate the serum. The analysis of specific cytokines, namely IFN-γ, TNF-α, IL-6, IL-10, and IL-1β, was performed using a Bio-Plex Pro Rat Cytokine 23-Plex Assay Kit (Bio-Rad) in accordance with the manufacturer's instructions.

Histology

Fresh liver and proximal colon tissue samples were immediately fixed by immersion in 4% paraformaldehyde solution for 24 hours at room temperature. Following standard dehydration and clearing procedures, the tissues were embedded in paraffin wax. Serial sections of 3–5 μm thickness were prepared using a rotary microtome. For histological examination, liver sections were subjected to Hematoxylin and Eosin (H&E) staining for general morphological assessment and Sirius Red staining for the specific detection of collagen deposits (fibrosis). Colon sections were stained with H&E for architectural evaluation.

DNA and RNA Extraction

Total DNA from rat fecal gut flora was extracted via a QIAamp Fast DNA Stool Mini Kit (Qiagen). Rat livers were extracted via a Qiagen RNeasy Plus Mini Kit (Qiagen). The integrity of the DNA and RNA was examined via agarose gel electrophoresis.

16S rRNA Gene Sequencing

PCR amplification of the V3-V4 region of the bacterial 16S rRNA gene was performed, and the selected universal primer sequences were 338F (5′-ACTCCTACGGGGAGGCAGCAG-3′) and 806R (5′- GGACTACHVGGGTWTCTAAT-3′). The PCR products were recovered and purified to construct a DNA library. The constructed DNA sequencing libraries were sequenced via an Illumina MiSeq paired-end sequencer (PE300). The sequences were divided and compared via QIIME and Vsearch software to select the appropriate operational taxonomic units (OTUs). α diversity was assessed by calculating the Simpson, Chao1 and Shannon indices via QIIME software (v1.9.1) to evaluate microbial diversity within each group. β diversity was assessed using QIIME software (v1.9.2) to calculate the microbial diversity within each group. β diversity was observed via principal coordinate analysis (PCoA) via QIIME software (v1.9.1) to observe the differences in microbial composition among the groups. Linear discriminant analysis effect size (LEfSe) was used to analyze differences in the abundance of flora and gene expression between groups. The analyses were considered statistically significant if the value of linear discriminant analysis (LDA) was greater than 2.5 or less than −2.5 and if the P value was less than 0.05.

Transcriptome Sequencing

Total RNA from liver tissues was used to construct paired-end (PE) sequencing libraries with the ABclonal mRNA-seq Lib Prep Module (for Illumina). Libraries were sequenced on an Illumina MiSeq platform in PE150 mode. Raw sequencing data in FASTQ format were quality-controlled and filtered using Fastp software. The clean reads were then aligned to the reference rat genome (mRn6) using HISAT2. Differential gene expression analysis was performed with the criteria of $|\log_2 (\text{fold change})| \geq 1$ and a q-value < 0.05. Gene Ontology (GO) and Kyoto Encyclopedia of Genes and Genomes (KEGG) pathway enrichment analyses were subsequently conducted on the identified differentially expressed genes (DEGs). The top 20 most significantly enriched KEGG pathways (based on p-value) were selected for visualization.

Statistical Analysis

All data in this experiment were analyzed via SPSS 20.0. All the data are expressed as the means ± SDs. First, the Shapiro–Wilk (S–W) test was used to determine whether the data were normally distributed. If normal distribution was observed, one-way analysis of variance (ANOVA) was used to compare differences among the three groups. Post hoc multiple comparisons between two groups were performed to determine if the data met the variance chi-square test; if the variance was found to be normal via chi-square test, a two-by-two comparison of the differences between the three groups was performed via post hoc comparison of least significant difference (LSD); if it was not found to be normal by chi-square, a two-by-two comparison of the differences between the two groups was performed via the Games-Howell test. If the data were not normally distributed, the nonparametric rank sum test (Kruskal–Wallis test) was used to analyze the difference between the three groups, and the Mann–Whitney *U*-test was used to compare the two groups that did not satisfy the normal distribution. $p < 0.05$ indicated that the difference in the data were statistically significant.

Results

F. Prausnitzii Attenuates Hepatic Abnormalities

As summarized in Table 1, rats with CCl_4-induced cirrhosis exhibited significantly elevated serum levels of ALT, AST, ALP, TB, DB, and GGT ($p < 0.05$, $p < 0.01$, $p < 0.001$), alongside a marked decrease in albumin (ALB) levels ($p < 0.001$) compared to the NC group, indicating severe hepatocyte damage and necrosis. Intervention with *F. prausnitzii* significantly ameliorated these alterations, leading to lower serum levels of ALT, AST, ALP, TB, and DB ($p < 0.05$, $p <$

Table 1 Comparison of Liver Function Indexes and Organ Coefficients in Different Groups of Rats (X±s)

	NC Group	CCL4 Group	*F. prausnitzii* Group
ALT	45.56±4.82*	319.08±175.56	77.92±16.57*
AST	165.07±15.67*	446.64±172.01	203.84±16.05*
ALB	34.54±0.59**	31.1±0.91	32.21±0.6*
ALP	93.71±24.17**	174.08±94.89	86.54±20.51**
TB	7.14±1.83*	13.51±3.59	8.12±2.47*
DB	3.47±0.98**	5.7±1.25	4.31±0.81
GGT	0.75±0.07*	0.88±0.07	0.77±0.12
Liver coefficient	0.28±0.002***	0.038±0.003	0.033±0.002**
Splenic index	0.019±0.005	0.0019±0.01	0.019±0.007

Notes: Data are expressed as mean ± standard deviation. (*p<0.05, **p<0.01, ***p<0.001).

0.01), a significant increase in ALB ($p < 0.05$), and a trend toward reduced GGT levels ($p = 0.051$). Furthermore, the liver index was significantly increased in the CCl_4 group ([0.038 ± 0.003] × 100%) compared to the NC group ([0.028 ± 0.002] × 100%), indicating hepatomegaly, which was significantly attenuated by *F. prausnitzii* treatment ([0.033 ± 0.002] × 100%). Collectively, these results demonstrate that *F. prausnitzii* attenuates liver function injury in cirrhotic rats.

F. Prausnitzii Attenuates Hepatic Fibrosis

Histopathological examination revealed extensive liver injury in the CCl_4 group, including substantial fibrous tissue proliferation in the interlobular areas, hepatocyte edema, degeneration and necrosis evidenced by numerous vacuoles, mild inflammatory cell infiltration, and grid-like collagen fiber deposition. These pathological manifestations were notably improved in the *F. prausnitzii*-treated group. As shown in Figure 2ii, microscopic analysis confirmed a reduction in the degree of liver fibrosis and connective tissue proliferation, although hepatic steatosis and vacuolization persisted. These findings indicate that *F. prausnitzii* administration slows the progression of liver fibrosis.

F. Prausnitzii Reduces the Serum Levels of Inflammatory Cytokines

Compared to the NC group, the CCl_4 group showed significantly elevated serum levels of the pro-inflammatory cytokines TNF-α, IL-6, IL-1β, and the anti-inflammatory cytokine IL-10 ($p < 0.05$, $p < 0.01$). *F. prausnitzii* treatment significantly reduced the serum levels of these inflammatory factors (TNF-α, IL-6, IL-10, IL-1β) compared to the CCl_4 group ($p < 0.05$, $p < 0.01$), although their levels remained higher than those in the NC group. Additionally, serum IFN-γ levels were

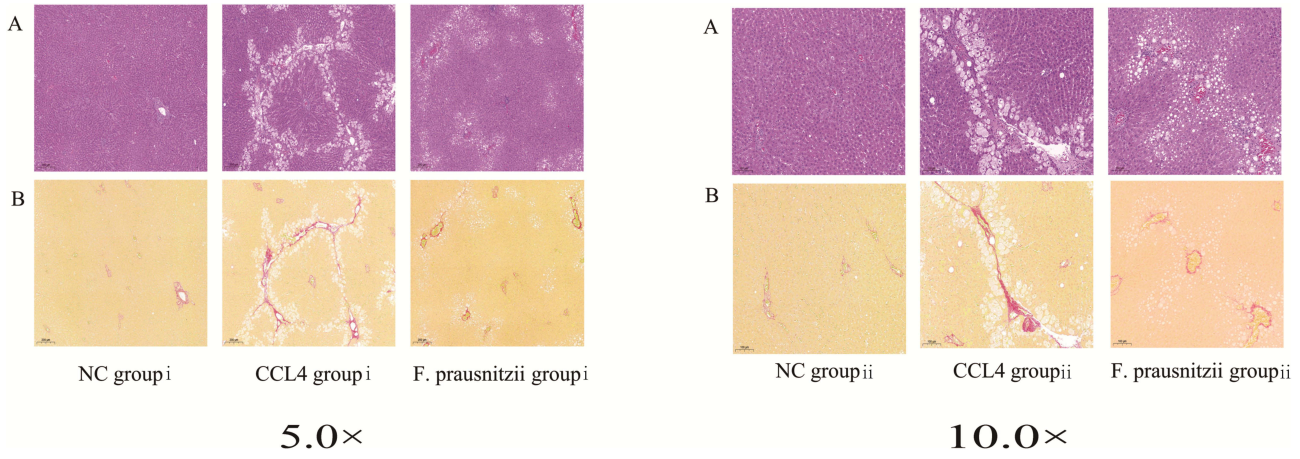

Figure 2 Histological sections of liver tissues in different groups. (**A**) Hematoxylin and eosin (HE) staining; (**B**) Sirius red staining. "i" represents the liver tissue pathology under a 5x microscope, and "ii" represents the liver tissue pathology under a 10x microscope.

https://doi.org/10.2147/CEG.S551412

significantly increased in the CCl_4 group ($p < 0.05$) and were significantly reduced by *F. prausnitzii* intervention ($p < 0.05$). In conclusion, *F. prausnitzii* administration effectively suppresses the systemic inflammatory response in CCl_4-induced cirrhotic rats. (Figure 3).

F. Prausnitzii Improves Intestinal Mucosal Barrier Function

Histopathological examination of colonic tissues (Figure 4) revealed severe intestinal mucosal damage in the CCl_4 group compared to the NC group, characterized by epithelial cell disruption, a reduced number of goblet cells, substantial inflammatory cell infiltration in the submucosa, and destruction of the villus architecture. In contrast, *F. prausnitzii* treatment markedly attenuated these injuries, resulting in less inflammatory cell infiltration and a more intact villus structure. These findings suggest that *F. prausnitzii* administration effectively preserves intestinal mucosal integrity and barrier function in cirrhotic rats.

F. Prausnitzii Improves the Intestinal Flora Structure

Analysis of the gut microbial community revealed significant alterations induced by CCl_4 and modulations by *F. prausnitzii* treatment. While the Shannon index was significantly higher in the CCl_4 group than in the NC group, no significant differences in overall microbial diversity were observed based on the Chao1 and Simpson indices (Figure 5). Principal

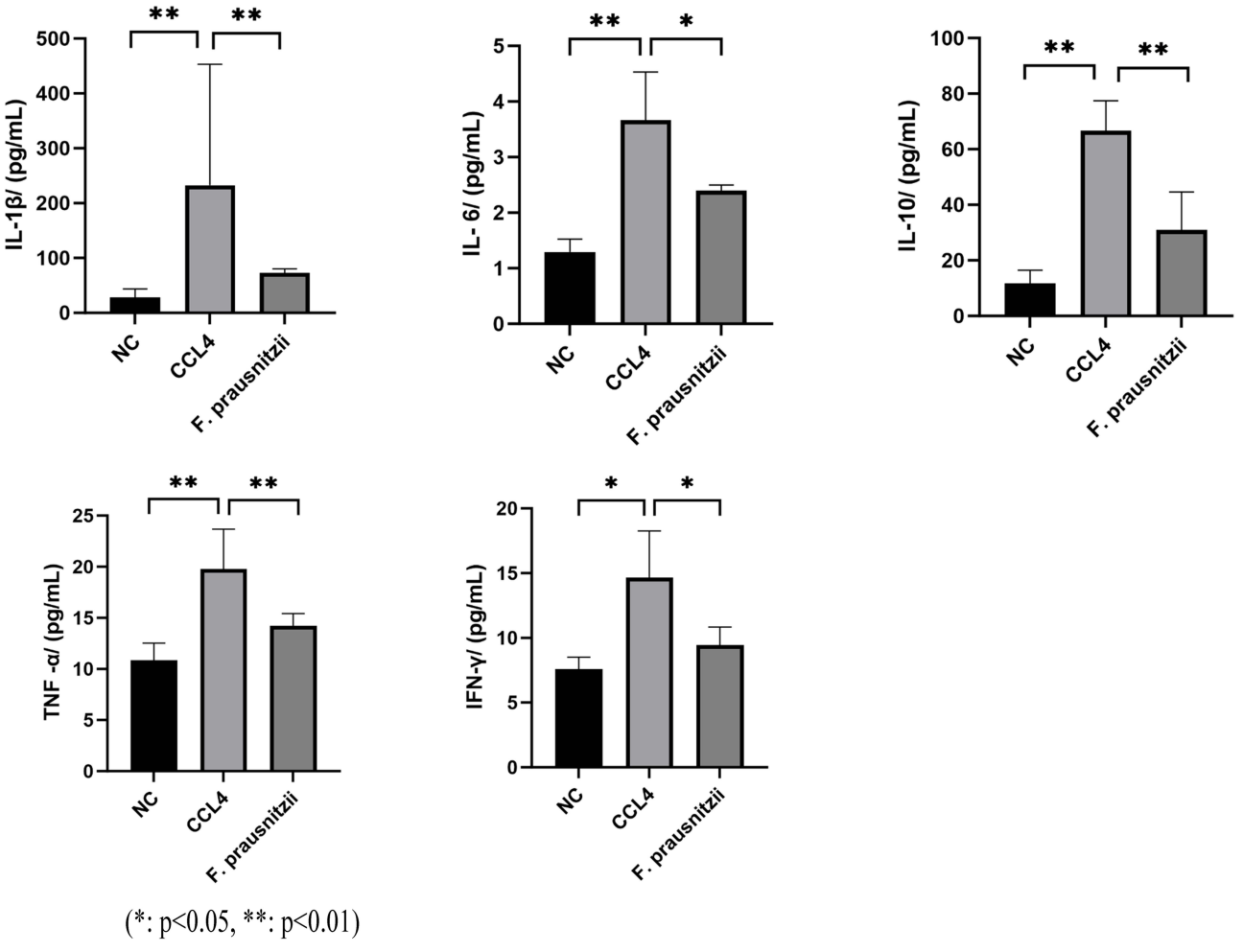

Figure 3 Bar graphs showing the effects of CCL4 and *F. prausnitzii* on inflammatory cytokines (IL-1β, IL-6, TNF-α, IL-10, IFN-γ) in a liver injury model. (*p<0.05, **p<0.01). **Abbreviations**: NC, Normal control group (untreated); CCL4, Carbon tetrachloride - treated group (induced liver injury); *F. prausnitzii, Faecalibacterium prausnitzii* - treated group (post - injury intervention).

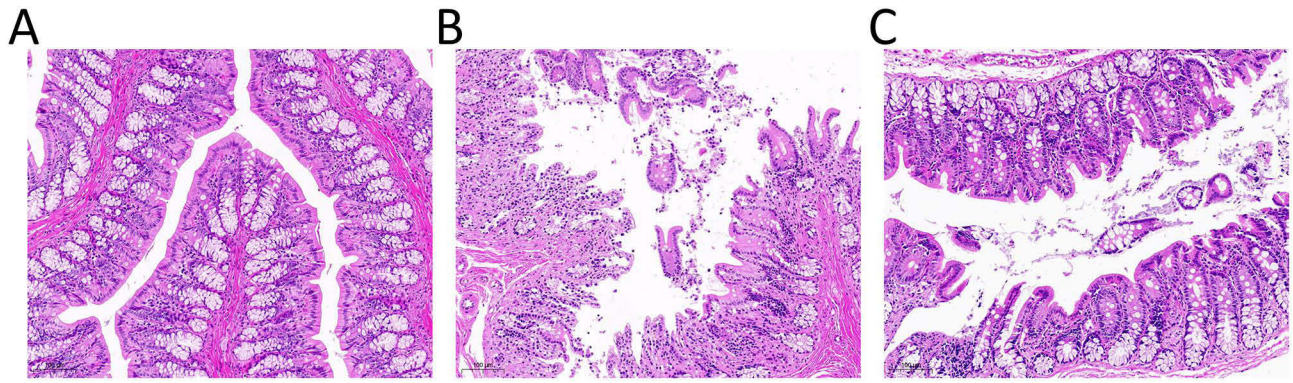

Figure 4 Histological sections of colorectal tissues at 10.0 magnification. This figure presents hematoxylin-eosin (H&E)-stained sections of colorectal tissues, illustrating the histological characteristics of three distinct groups: (**A**) control group; (**B**) CCL4 group: epithelial cells and goblet cells were reduced, and villi were destroyed; (**C**) After treatment with F. prausnitzii, the epithelial cells, goblet fineness and villi destruction of cirrhotic mice were reduced than before.

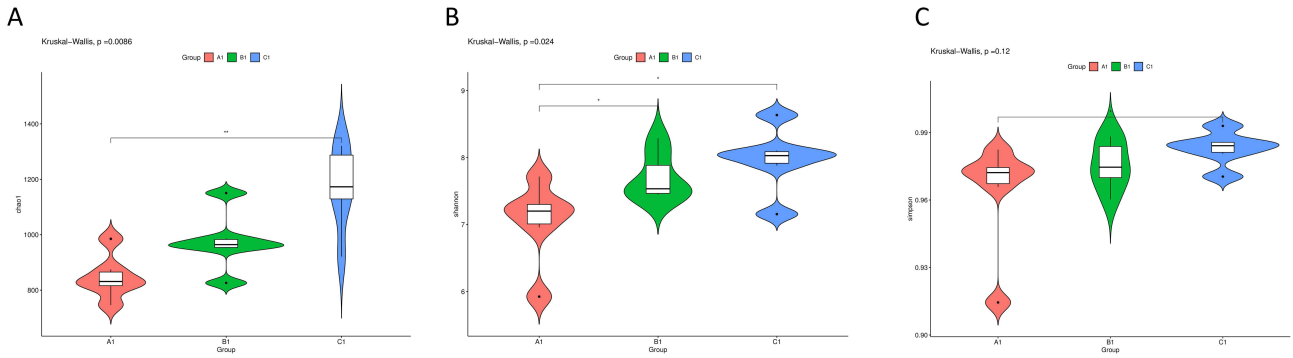

Figure 5 Violin plots of microbial diversity indices in three groups (A1—NC group, B1—CCL4 group, C1—F. prausnitzii group). (**A**) chao1 index indicated that compared with A1 of control group, intestinal flora of test group B1 and C1 had different changes; (**B**) shannon index revealed that there was no significant difference in overall microbial diversity between B1 and C1. (**C**) The results revealed by Simpson index are roughly consistent with the shannon index. (*p<0.05, **p<0.01).

coordinate analysis (PCoA) based on unweighted UniFrac distances revealed distinct clustering, indicating significant differences in microbial community structures among the CCl_4, *F. prausnitzii*, and NC groups (Figure 6A).

Significant variations in microbial taxonomic abundance were observed at both the phylum and genus levels (Figure 6B). At the phylum level, the CCl_4 group exhibited a significant increase in the abundances of *Firmicutes* and *Verrucomicrobiota* and a decrease in *Bacteroidota* compared to the NC group. *F. prausnitzii* treatment reversed these changes, significantly reducing the relative abundances of *Firmicutes* and *Verrucomicrobiota* and increasing the abundance of *Bacteroidota*.

At the genus level, the CCl_4 group was enriched in *Lachnospiraceae NK4A136, Firmicutes*, and *Akkermansia*, while the abundances of *Lactobacillus, UCG-005*, and *Escherichia/Shigella* were significantly decreased compared to the NC group. *F. prausnitzii* intervention significantly increased the abundances of *Lactobacillus* and *UCG-005* and decreased the abundances of *Akkermansia, Rhodococcus*, and *Pseudoalteromonas* compared to the CCl_4 group.(Figure 6C).

LEfSe analysis further identified specific taxa that were enriched in each group (Figure 7). The NC group was predominantly enriched in *Lactobacillus, UCG-005, Coriobacteriaceae, Collinsella, Escherichia/Shigella*, and *Rhodoferax*. The CCl_4 group was characterized by enrichments in *Verrucomicrobiota, Akkermansia, Eubacterium ruminantium, Nocardiaceae, Rhodococcus, Corynebacteriales, Pseudoalteromonas*, and *Kineothrix*. The *F. prausnitzii* group was mainly enriched in *Lachnospiraceae, Firmicutes*, and *Turicibacter*.

https://doi.org/10.2147/CEG.S551412

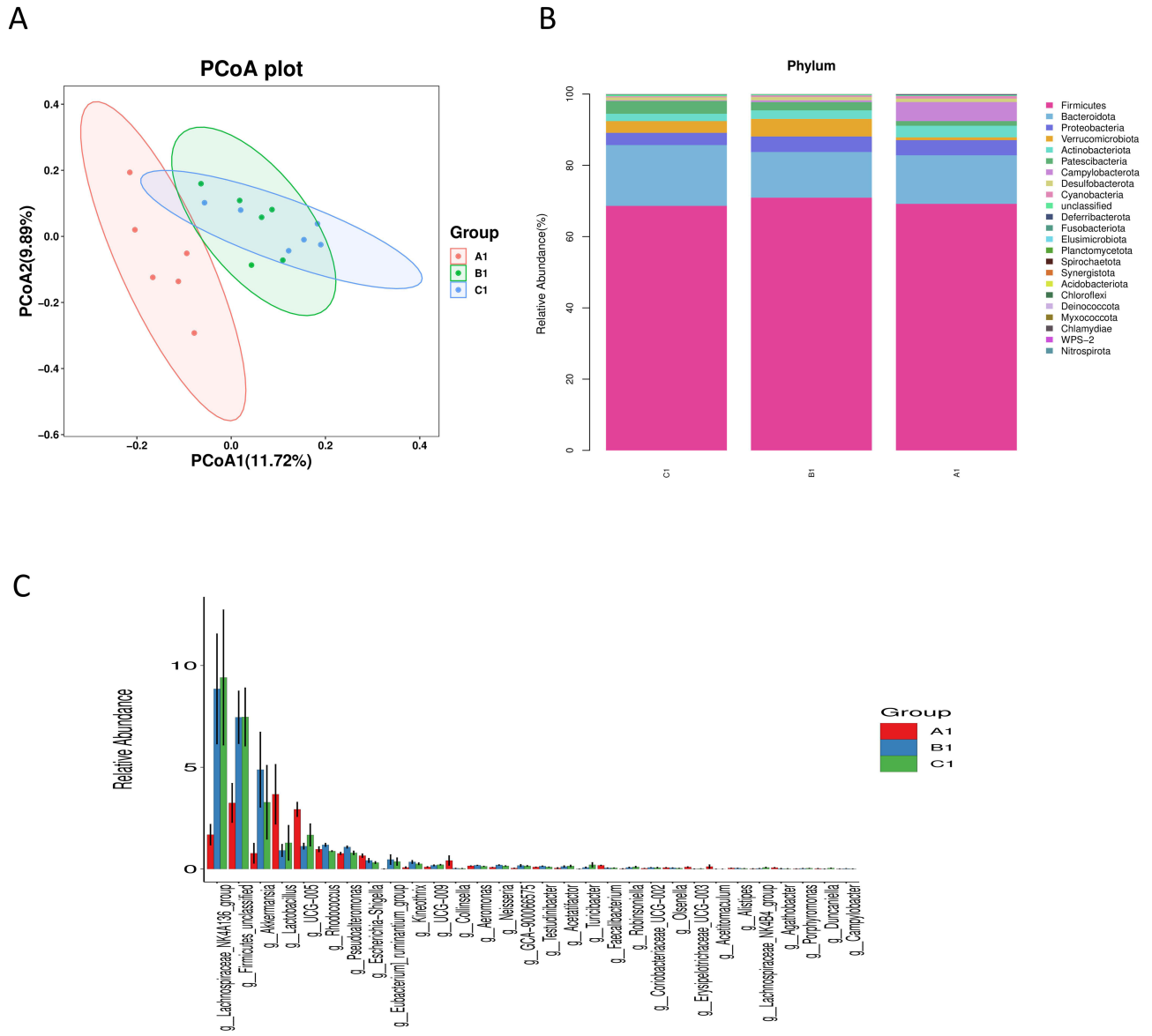

Figure 6 Microbial community composition across experimental groups. (A1—NC group, B1—CCL4 group, C1—F. prausnitzii group). (**A**) Principal coordinate analysis (PCoA) based on unweighted UniFrac distances, showing distinct clustering of the microbial communities for each group (A1, B1, C1). (**B**) Phylum-level relative abundance profile. The stacked bar plot displays the compositional differences in major bacterial phyla among the groups. (**C**) Genus-level relative abundance of the most abundant taxa. The bar plot compares the abundances of top-ranked genera across groups.

F. Prausnitzii Modulates Transcriptome Expression

Transcriptomic profiling of liver tissues identified substantial gene expression alterations associated with CCl_4-induced cirrhosis and *F. prausnitzii* intervention. A total of 566 differentially expressed genes (DEGs) were identified in the CCl_4 group compared to the NC group, with 486 upregulated and 80 downregulated (Figure 8). Treatment with *F. prausnitzii* significantly modulated this expression profile, resulting in 239 DEGs compared to the CCl_4 group (176 upregulated and 63 downregulated). Hierarchical clustering clearly distinguished the transcriptomic patterns among the three groups (Figures 8C and 9D).

Functional enrichment analysis of the DEGs between the CCl_4 and NC groups revealed significant insights (Figure 9A and B). Gene Ontology (GO) analysis highlighted enrichment in biological processes such as positive regulation of transcription by RNA polymerase II, oxidation-reduction process, and signal transduction. At the cellular component level, genes were predominantly localized to the membrane, cytoplasm, and nucleus. Molecular functions were chiefly associated with protein

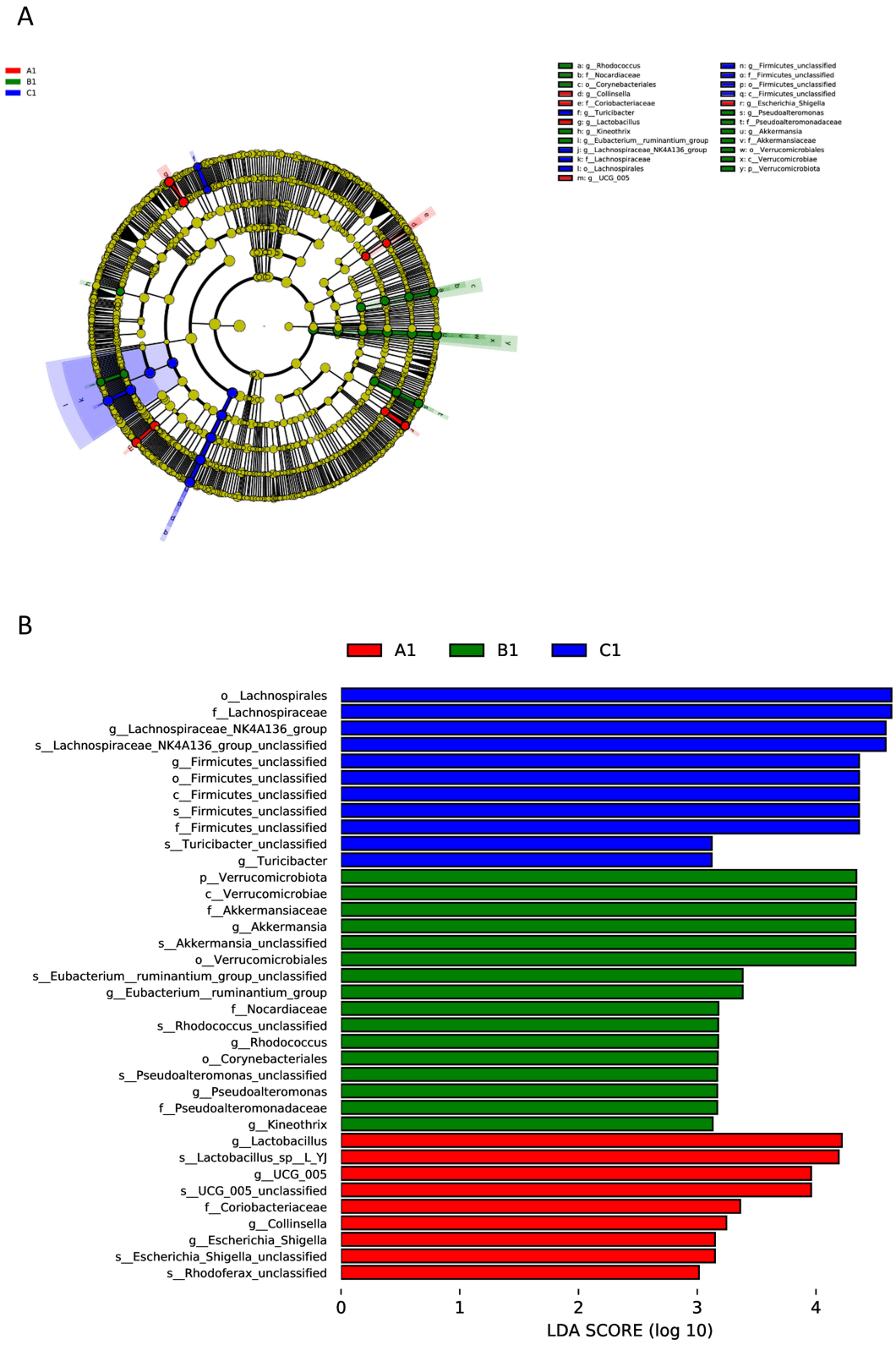

Figure 7 Phylogenetic distribution and differential abundance of gut microbiota across groups. (A1—NC group, B1—CCL4 group, C1—F. prausnitzii group). (**A**) Circular phylogenetic tree depicting the evolutionary relationships and relative abundance of microbial taxa. The tree is colored by phylogenetic classification (phylum level), and node sizes correspond to taxon abundance. The outer ring highlights group-specific distributions (A1, red; B1, green; C1, blue). (**B**) Linear discriminant analysis effect size (LEfSe) results showing taxa with the most significant differences in abundance between groups. Bars represent the LDA score (log10-transformed), indicating the effect size of each differentially abundant taxon. Taxa are colored according to the group in which they are most enriched.

https://doi.org/10.2147/CEG.S551412

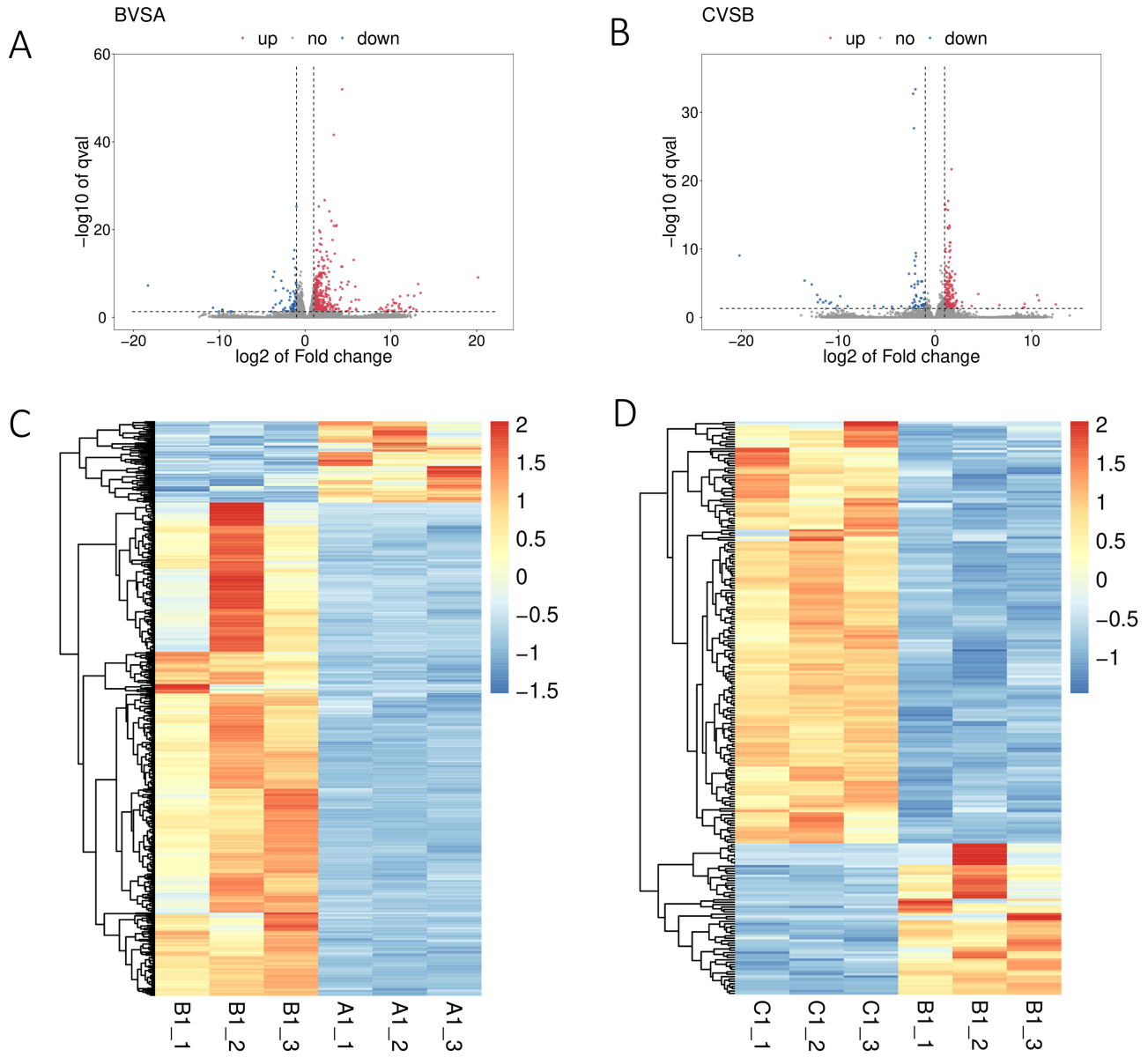

Figure 8 Transcriptomic analysis of gene expression differences among A1, B1and C1 (A1—NC group, B1—CCL4 group, C1—F. prausnitzii group). (**A**) Describe the results of differential expression analysis among the three groups in the BVSA data; (**B**) Describe the differential expression analysis results among the three groups in the CVSB data; (**C**) Heat maps showed the change of gene expression between A1 and B1; (**D**) Heat maps showed changes in gene expression between B1 and C1.

binding, metal ion binding, and ATP binding. KEGG pathway analysis further indicated significant involvement of protein processing in the endoplasmic reticulum, metabolism of xenobiotics by cytochrome P450, cholesterol metabolism, bile secretion, and the PPAR signaling pathway.

Notably, *F. prausnitzii* administration induced a distinct functional shift (Figure 9C and D). GO analysis of the DEGs in the *F. prausnitzii* group versus the CCl_4 group showed enrichment in monoatomic ion transport, the G protein-coupled receptor signaling pathway, and protein phosphorylation. KEGG pathway analysis underscored a pronounced impact on neuroactive ligand-receptor interaction and multiple neural and signaling pathways, including calcium signaling, cAMP signaling, glutamatergic synapse, and dopaminergic synapse.

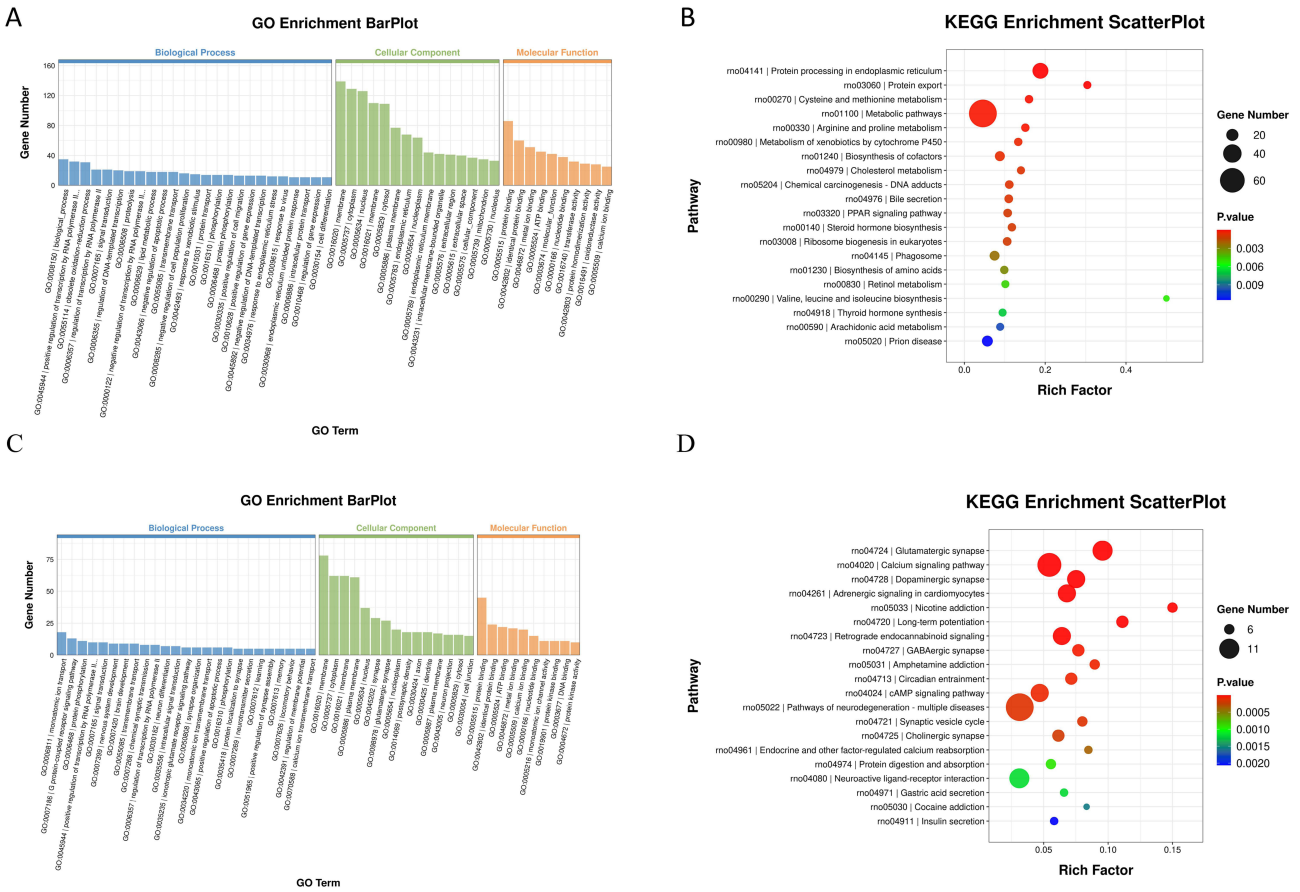

Figure 9 Functional enrichment analysis diagram. (**A** and **B**) GO function analysis and KEGG pathway analysis of CCL4 compared with NC group; (**C** and **D**) GO function analysis and KEGG pathway analysis of *F. prausnitzii* group compared with CCL4 group.

Discussion

Our findings demonstrate that *F. prausnitzii* administration ameliorates CCl_4-induced liver cirrhosis in rats by orchestrating a multi-faceted repair program via the gut-liver axis. The therapeutic effects are manifested as improved liver function, attenuated fibrosis, reduced systemic inflammation, restored gut microbiota balance, and enhanced intestinal barrier integrity, ultimately leading to the mitigation of cirrhotic pathology.

The serum levels of AST and ALT are considered markers of liver injury,[13] while bilirubin and albumin levels reflect the liver's metabolic and synthetic function. In the present study, cirrhotic rats treated with *F. prausnitzii* presented significant improvements in these critical parameters. The significant reduction in these classic serum markers and the increase in ALB collectively indicate a fundamental improvement in hepatocellular integrity and synthetic function, which are central to halting and reversing the progression of cirrhosis. This was further corroborated by our pathological results, which revealed a noticeable reduction in hepatocyte damage.

Cirrhosis develops as a result of persistent inflammation and liver injury.[14] The upregulation of proinflammatory cytokines such as TNF-α, IL-1β, and IL-6 leads to hepatocyte necrosis and promotes the development of liver fibrosis.[15] Our results revealed that *F. prausnitzii* administration significantly decreased the levels of these key pro-inflammatory mediators. Notably, we also observed a marked increase in the anti-inflammatory cytokine IL-10 in the *F. prausnitzii* treatment group. This finding is mechanistically coherent: butyrate, a primary metabolite of F. prausnitzii, is a known potent inducer of IL-10 secretion from regulatory T cells and macrophages.[16] Therefore, the concurrent suppression of pro-inflammatory cytokines and induction of IL-10 represents a dual, complementary anti-inflammatory mechanism through which *F. prausnitzii* restores immune homeostasis. Since sustained hepatic inflammation is a primary driver of

https://doi.org/10.2147/CEG.S551412

hepatic stellate cell (HSC) activation, the rectification of this pro-inflammatory milieu by *F. prausnitzii* directly contributes to the retardation of fibrogenesis (Figure 2i).

The close relationship between the intestinal flora and the liver, termed the gut-liver axis, is well-established. Liver disease is consistently accompanied by intestinal dysbiosis.[17,18] In our model, this was characterized by a significantly increased Firmicutes/Bacteroidota (F/B) ratio, a hallmark signature of dysbiosis in metabolic and liver diseases.[19,20] We demonstrate that *F. prausnitzii* intervention effectively restructured the gut microbiota towards a healthier state, as evidenced by the reversal of specific cirrhosis-associated dysbiotic features: First, it normalized the F/B ratio, a primary indicator of ecosystem stability. Second, it induced a functional shift in the microbial community by significantly increasing the abundance of recognized beneficial genera, including the probiotic Lactobacillus and the short-chain fatty acid (SCFA) producer UCG-005. Concurrently, it suppressed genera potentially detrimental in this context, such as Rhodococcus and Pseudoalteromonas. The reduction of Akkermansia,[21] while often beneficial in healthy states, may reflect a positive normalization here, as its overgrowth in a compromised gut can exacerbate mucosal barrier degradation. Critically, this compositional restoration is functionally meaningful. The enrichment of SCFA producers is pivotal, as SCFAs—particularly butyrate—are known to reinforce the intestinal barrier, reduce bacterial translocation, and exert direct anti-inflammatory effects on the liver.[10] This proposed mechanism is strongly supported by our correlative histological evidence of improved colonic mucosa structure (Figure 4), indicating a strengthened defense against gut-derived toxins. Therefore, the collective reversal of dysbiotic signatures, coupled with the promotion of a SCFA-producing community, provides a compelling rationale for our claim that the microbiota structure was functionally improved following *F. prausnitzii* administration.

To gain deeper mechanistic insight, we investigated the hepatic transcriptomic changes. KEGG enrichment analysis highlighted the retinol and arachidonic acid metabolism pathways. The downregulation of the retinol metabolism pathway in the *F. prausnitzii* group is particularly relevant, as aberrant retinoic acid signaling has been implicated in promoting HSC activation and the fibrotic response in chronic liver injury.[22] Our data suggest that *F. prausnitzii* may interrupt this pro-fibrotic signaling axis. Similarly, the normalization of arachidonic acid metabolism pathway activity likely contributes to reduced inflammation. Overproduction of arachidonic acid-derived eicosanoids exacerbates portal hypertension and liver inflammation.[23] *F. prausnitzii*-mediated mitigation of this pathway aligns with the observed reduction in inflammatory cytokines and suggests an improvement in the hepatic hemodynamic profile.[24] While these transcriptomic findings provide strong, hypothesis-generating insights, future studies incorporating metabolomic analysis will be crucial to directly quantify the shifts in retinoic acid and eicosanoid metabolites, thereby solidifying these mechanistic claims.

In conclusion, we propose a cohesive mechanism for the beneficial effects of *F. prausnitzii* in cirrhotic rats: *F. prausnitzii* restores gut microbial homeostasis, enriching SCFA-producing bacteria. The subsequent increase in butyrate strengthens the intestinal mucosal barrier, reducing the influx of gut-derived pathogens and inflammatory stimuli into the portal circulation. This alleviates the chronic inflammatory burden on the liver, leading to reduced activation of HSCs and dampened pro-fibrotic signaling pathways (eg, retinol metabolism). Consequently, hepatocellular damage is minimized, liver function is recovered, and the progression of fibrosis is halted. Thus, our study firmly establishes *F. prausnitzii* as a promising probiotic therapeutic agent that targets the gut-liver axis to mitigate the complex pathophysiology of cirrhosis.

This study has several limitations that warrant consideration. First, our findings are derived from an acute CCl_4-induced cirrhosis model, which, while well-established, does not fully replicate the complex, multi-factorial etiology (eg, viral, alcoholic, metabolic) and slow, chronic progression characteristic of human cirrhosis. This difference may affect the direct clinical translatability of our findings. Second, the sample size, though adequate for this preliminary investigation, remains relatively modest; future studies with larger cohorts are needed to strengthen the statistical power and generalizability of our conclusions. Third, a key methodological limitation is the use of live F. prausnitzii. This precludes definitive conclusions on whether the observed therapeutic benefits were mediated by the bacteria themselves (via colonization or nutritional competition), their metabolites, or a combination thereof. While our correlative data (eg, elevated butyrate levels and supportive transcriptomic changes) suggest a significant role for bacterial metabolites, future studies employing control groups such as heat-killed *F. prausnitzii* and its culture supernatant are

essential to dissect the precise mechanisms. Fourth, our ability to directly quantify the colonization efficiency of the administered *F. prausnitzii* strain is constrained by the methodological limitations of 16S rRNA sequencing, which cannot reliably distinguish exogenous from indigenous populations at the strain level. The significant microbial restructuring and functional improvements observed provide compelling indirect evidence of its establishment and activity, but future studies utilizing strain-specific tracking methods are warranted for conclusive quantification. Finally, as previously acknowledged, the histological assessment could have been strengthened by employing a semi-quantitative fibrosis scoring system (eg, Ishak or METAVIR), which would have provided more precise morphological quantification.

Despite these limitations, our study comprehensively demonstrated the therapeutic potential of *F. prausnitzii* through a multidimensional approach. Further research in more chronic and clinically relevant models, with expanded sample sizes, specifically designed control groups, and advanced microbial tracking techniques, is essential to validate these promising results and robustly explore their applicability to human disease.

Conclusion

In summary, our study demonstrates that *F. prausnitzii* supplementation alleviates the progression of cirrhosis in rats through a multi-targeted mechanism. It effectively attenuates liver injury and fibrosis, modulates the systemic inflammatory response, restores gut microbiota homeostasis, and enhances intestinal barrier integrity. These beneficial effects are further associated with the regulation of key metabolic pathways, including arachidonic acid and retinol metabolism, in the liver. Our findings underscore the critical role of the gut-liver axis in liver health and highlight the promising potential of targeting the gut microbiota, particularly with *F. prausnitzii*, as a novel therapeutic strategy for the management of cirrhosis.

Ethics Approval and Consent to Participate

All methods were carried out in accordance with relevant guidelines and regulations. The study was approved by the Ethics Committee of the First Affiliated Hospital, College of Clinical Medicine, Henan University of Science and Technology (2019G-015).

Author Contributions

All authors made a significant contribution to the work reported, whether that is in the conception, study design, execution, acquisition of data, analysis and interpretation, or in all these areas; took part in drafting, revising or critically reviewing the article; gave final approval of the version to be published; have agreed on the journal to which the article has been submitted; and agree to be accountable for all aspects of the work.

Funding

This study was sponsored by Science and technology Research program of Henan Province, (NO 212102310191) and Henan Province Medical Science and technology Research joint project (NO LHGJ20230472).

Disclosure

The authors declare no competing interests in this work.

References

1. Paul Starr S, Raines D. Cirrhosis: diagnosis, management, and prevention. *Am Family Phys*. 2011;84:1353.
2. Asrani SK, Devarbhavi H, Eaton J, et al. Burden of liver diseases in the world. *J Hepatol*. 2019;70:151–171. doi:10.1016/j.jhep.2018.09.014
3. Bhat M, Arendt BM, Bhat V, et al. Implication of the intestinal microbiome in complications of cirrhosis. *World J Hepatol*. 2016;8:1128–1136. doi:10.4254/wjh.v8.i27.1128
4. Qin N, Yang F, Li A, et al. Alterations of the human gut microbiome in liver cirrhosis. *Nature*. 2014;513:59–64. doi:10.1038/nature13568
5. Milosevic I, Vujovic A, Barac A, et al. Gut-liver axis, gut microbiota, and its modulation in the management of liver diseases: a review of the literature. *Nat Rev Neurosci*. 2019;20:30.
6. Fukui H, Tomita T, Tozawa K, Oshima T, Fukui H, Miwa H. Leaky gut and gut-liver axis in liver cirrhosis: clinical studies update. *Gut Liver*. 2020;14:281–290. doi:10.5009/gnl19079

7. Bajaj JS, Heuman DM, Hylemon PB, et al. Altered profile of human gut microbiome is associated with cirrhosis and its complications. *J Hepatol*. 2014;60:940–947. doi:10.1016/j.jhep.2013.12.019
8. Usami M, Miyoshi M, Yamashita H. Gut microbiota and host metabolism in liver cirrhosis. *World J Gastroenterol*. 2015;21:11597–11608. doi:10.3748/wjg.v21.i41.11597
9. Heinken A, Khan MT, Paglia G, et al. Functional metabolic map of faecalibacterium prausnitzii, a beneficial human gut microbe. *J Bacteriol*. 2014;196:3289–3302. doi:10.1128/JB.01780-14
10. Miquel S, Martín R, Rossi O, et al. Faecalibacterium prausnitzii and human intestinal health. *Curr Opin Microbiol*. 2013;16:255–261. doi:10.1016/j.mib.2013.06.003
11. Huang XL, Zhang X, Fei XY, et al. Faecalibacterium prausnitzii supernatant ameliorates dextran sulfate sodium induced colitis by regulating Th17 cell differentiation. *World J Gastroenterol*. 2016;22:5201–5210. doi:10.3748/wjg.v22.i22.5201
12. Zhang M, Zhou Q, Dorfman RG, et al. Butyrate inhibits interleukin-17 and generates Tregs to ameliorate colorectal colitis in rats. *BMC Gastroenterol*. 2016;16:84. doi:10.1186/s12876-016-0500-x
13. Sookoian S, Pirola CJ. Liver enzymes, metabolomics and genome-wide association studies: from systems biology to the personalized medicine. *World J Gastroenterol*. 2015;21:711.
14. Pratim DP, Medhi S. Role of inflammasomes and cytokines in immune dysfunction of liver cirrhosis. *Cytokine*. 2023;170:156347.
15. Kany S, Vollrath JT, Relja B. Cytokines in Inflammatory Disease. *Int J Mol Sci*. 2019;20:6008. doi:10.3390/ijms20236008
16. Martín R, Miquel S, Benevides L, et al. Functional characterization of novel faecalibacterium prausnitzii strains isolated from healthy volunteers: a step forward in the use of f. prausnitzii as a next-generation probiotic. *Front Microbiol*. 2017;8:1226. doi:10.3389/fmicb.2017.01226
17. Habermaass V, Olivero D, Gori E, et al. Intestinal microbiome in dogs with chronic hepatobiliary disease: can we talk about the gut-liver axis? *Animals*. 2023:13. doi: 10.3390/ani13203174
18. Wang R, Tang R, Li B, et al. Gut microbiome, liver immunology, and liver diseases. *Cell Mol Immunol*. 2020;18:4–17.
19. Yang T, Santisteban MM, Rodriguez V, et al. Gut dysbiosis is linked to hypertension. *Hypertension*. 2015;65:1331–40.
20. Sanz Y, Moya-Pérez A. Microbiota, inflammation and obesity. *Adv Exp Med Biol*. 2014;817:291–317.
21. Zhang J, Guo Z, Xue Z, et al. A phylo-functional core of gut microbiota in healthy young Chinese cohorts across lifestyles, geography and ethnicities. *Isme J Multidiscip J Microbial Ecol*. 2015;9:1979–1990.
22. Chen M, Liu J, Yang W, et al. Lipopolysaccharide mediates hepatic stellate cell activation by regulating autophagy and retinoic acid signaling. *Autophagy*. 2017;13:1813–1827. doi:10.1080/15548627.2017.1356550
23. Joshi V, Umashankara M, Ramakrishnan C, et al. Dimethyl ester of bilirubin exhibits anti-inflammatory activity through inhibition of secretory phospholipase A2, lipoxygenase and cyclooxygenase. *Arch Biochem Biophys*. 2016;598:28–39. doi:10.1016/j.abb.2016.04.003
24. Pettinelli P, Arendt BM, Schwenger KJP, et al. Relationship between hepatic gene expression, intestinal microbiota, and inferred functional metagenomic analysis in NAFLD. *Clin Transl Gastroenterol*. 2022;13:e00466. doi:10.14309/ctg.0000000000000466